NanoSail – D Orbital and Attitude Dynamics

Andrew F. Heaton[1]
NASA Marshall Space Flight Center, Huntsville, AL 35812

Brent F. Faller [2] and Chelsea K. Katan [3]

Embry-Riddle Aeronautical University, Prescott, AZ 86301

NanoSail-D unfurled January 20th, 2011 and successfully demonstrated the deployment and deorbit capability of a solar sail in low Earth orbit. The orbit was strongly perturbed by solar radiation pressure, aerodynamic drag, and oblate gravity which were modeled using STK HPOP. A comparison of the ballistic coefficient history to the orbit parameters exhibits a strong relationship between orbital lighting, the decay rate of the mean semi-major axis and mean eccentricity. A similar comparison of mean solar area using the STK HPOP solar radiation pressure model exhibits a strong correlation of solar radiation pressure to mean eccentricity and mean argument of perigee. NanoSail-D was not actively controlled and had no capability on-board for attitude or orbit determination. To estimate attitude dynamics we created a 3-DOF attitude dynamics simulation that incorporated highly realistic estimates of perturbing forces into NanoSail-D torque models. By comparing the results of this simulation to the orbital behavior and ground observations of NanoSail-D, we conclude that there is a coupling between the orbit and attitude dynamics as well as establish approximate limits on the location of the NanoSail-D solar center of pressure. Both of these observations contribute valuable data for future solar sail designs and missions.

[1] Senior Aerospace Engineer, EV42/ Guidance, Navigation and Mission Analysis, NASA Marshall Space Flight Center.

[2] Fall Semester 2012 Intern, EV42/Guidance, Navigation and Mission Analysis, NASA Marshall Space Flight Center.

[3] Spring Semester 2012 Intern, EV42/Guidance, Navigation and Mission Analysis, NASA Marshall Space Flight Center.

Nomenclature

β	=	angle between sun-earth line and orbit plane
e	=	eccentricity
AOP	=	Argument of Perigee
I	=	inertia tensor
α	=	angular attitude [deg]
ω	=	angular velocity [deg s^{-1}]
τ	=	torque [N m]
ρ	=	density [kg m^3]
v	=	velocity [m s^{-1}]
Cd	=	drag co-efficient
A	=	sail drag area [m^2]
S	=	total sail area [m^2]
We	=	solar constant [J s^{-1} m^{-2}]
c	=	speed of light in vacuum [m s^{-1}]
r_e	=	distance of earth from sun [km]
r_s	=	distance of satellite from sun [km]
k	=	gravitational constant
R	=	semi-major axis [km]
I_{xx}	=	inertial moment about x-axis
I_{yy}	=	inertial moment about y-axis
I_{zz}	=	inertial moment about z-axis
a_x	=	direction cosine of x-axis in body frame
a_y	=	direction cosine of x-axis in body frame
a_z	=	direction cosine of x-axis in body frame

I. Introduction

NanoSail-D was released from the NASA FASTSAT-HSV01 satellite on January 17, 2011 and unfurled three days later on January 20 to become the first American solar sail deployed in space [1]. NanoSail-D (NSD) successfully demonstrated deployment of a solar sail in Low Earth Orbit (LEO) and stayed on orbit nearly nine months, re-entering on September 17, 2011. NSD had no active control capability and no onboard instrumentation to determine attitude or position, so ground observations were the sole source of flight data. These observations included orbit estimates in the form of Two Line Element (TLE) sets as well as a few ground-based visual observations that provided rough estimates of spin rate and limited insight into the attitude. Our goal in this research is to use the limited set of flight data to construct a time history of the ballistic coefficient based on orbit decay, attempt to model the effect of orbital lighting, and seek insight into the attitude dynamics of the NSD with an emphasis on bounding the location of the Center of Pressure (CP) of the solar force on the sail. In addition to the demonstration of solar sail technology, NSD also had a flight objective to demonstrate its utility as a de-orbit device [2] and this objective was clearly demonstrated.

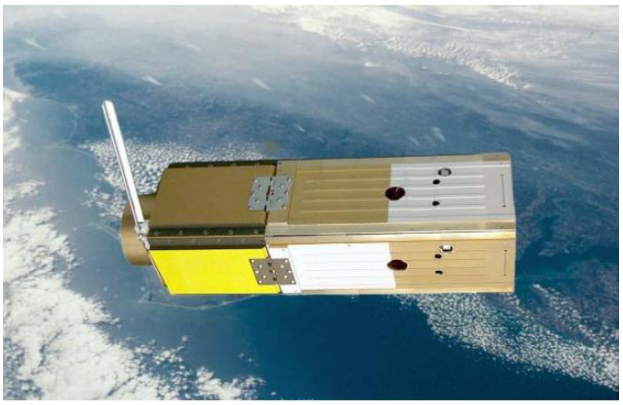

Fig. 1 NanoSail-D Cubesat Prior to Deploy

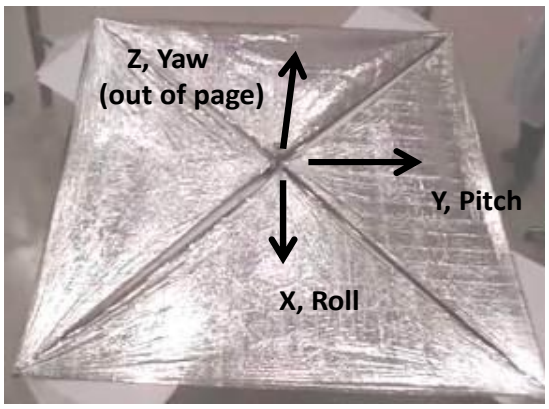

Fig. 2 NanoSail-D Deployed in Ground Test

II. Background

NSD was a 10 square meter sail deployed from a 3U Cubesat as depicted in Fig. 1. Fig. 2 shows the deployed sail during a ground test. Note in Fig. 2 that the X and Y axes are symmetric and located in the sail plane. From this, we can observe that the sail is axisymmetric about the Z axis which implies a potential for spin-stability about

that axis. The sail structure consisted of four thin triangular sheets of aluminized CP-1 material attached to four Triangular Rollable and Collapsible (TRAC) booms as depicted in Fig. 3. Each triangle of the sail is mounted to two TRAC boom ends, each 2.2 m. long, and the bus. The TRAC booms depicted in Fig. 3 were collapsed inside the cube satellite before launch and deployed the sail in approximately five seconds in space.

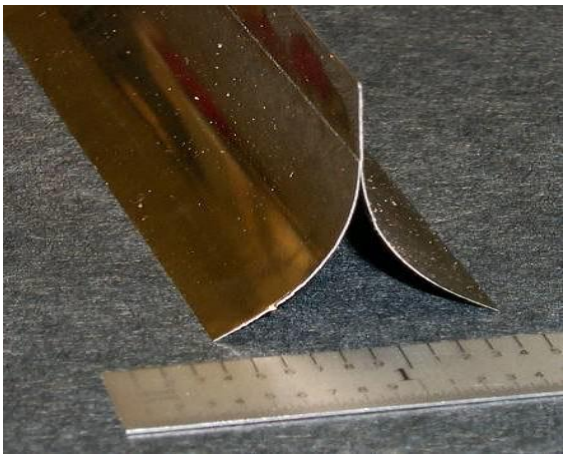

Fig. 3 TRAC Boom

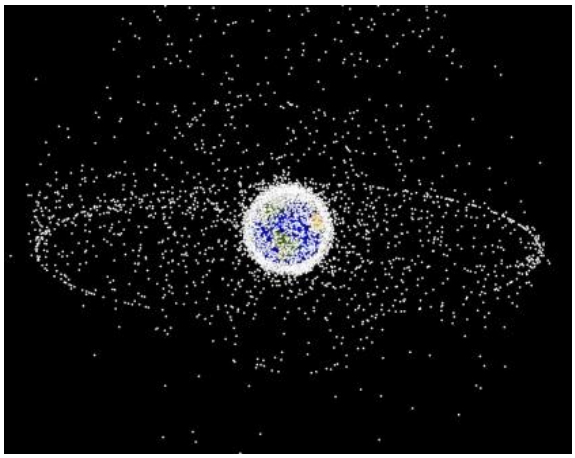

Fig. 4 Space Junk Orbiting Earth

NSD was inserted into a 71.9 degree inclination orbit at an altitude of 654 km. At this high inclination, full sun occurred periodically during the 9 months the sail was on orbit. The orbit decayed swiftly in spite of the high initial altitude due to the high area/mass ratio of the NSD.

NASA developed the Solar Sail Spaceflight Simulation Software (S5) [3,4] to model all aspects of interplanetary solar sail missions, but since Low Earth Orbit (LEO) is not generally considered a good mission fit for solar sails, S5 does not currently include atmospheric models. Thus for the orbit decay analysis we used Systems Tool Kit (STK) High Precision Orbit Propagator (HPOP) to determine the time history of the ballistic coefficient. The default Solar Radiation Pressure (SRP) model in STK HPOP was also used to model the SRP effect on the orbit and was compared to higher fidelity models in S5 over relatively short simulation time periods. Since the flight data available for inclusion into the various simulations was rather limited in accuracy, the relative lack of fidelity in the SRP model in STK HPOP was not an important issue in the analysis and STK HPOP was the primary simulation for the orbit dynamics. To model NSD attitude dynamics we created a new Matlab 3-Degree-Of-Freedom (3-DOF) rigid body dynamics simulation.

One of the objectives of NSD was to demonstrate that a sail can be used to de-orbit space junk. More than 521,000 human-made defunct devices greater than 1 cm in diameter now orbit Earth at velocities up to 8 km/s (see Fig. 4). Many pose an impact danger to operational satellites and the International Space Station. Thus the demonstration of the potential of a sail-like device for rapid de-orbit of space junk is strong ancillary benefit of the NSD mission.

III. Analysis

Given the lack of detailed mission data, the challenge was to extract as much useful information as possible from what was available. We started by identifying what was well known and proceeding to incorporate the lower-fidelity data sets. The best-characterized set of data was the orbit history consisting of Two Line Element (TLE) state vectors. Although the TLE vectors have a known limit of accuracy, the frequency with which they were updated allowed an orbit determination more than sufficient to characterize the time history of the ballistic coefficient of the NSD.

Solar radiation perturbations in LEO tend to affect eccentricity and argument of perigee more than the other orbital elements [5]. Thus we modeled the orbit with and without a Solar Radiation Pressure (SRP) model to determine whether the SRP effects on these two parameters could be isolated. For this analysis we used the baseline SRP model in STK, which is the spherical model. The spherical SRP model aligns the solar force completely along sun-spacecraft line, which means that it was essentially like a flat plate pointed directly at the Sun with no attitude variations possible. However, since from ground observations we know that NSD was rotating much more rapidly than the orbital period, an assumption can be made that NSD over the course of an orbit points an “average solar area” at the sun that is a flat plate equivalent. In the same way that the ballistic coefficient can be varied, one can then use the spherical SRP model in STK as a “solar ballistic coefficient” area. The SRP model can then be fitted as an average solar area as the orbital geometry (and spin axis of the NSD) evolves over time.

The analysis also included the creation of a 3-Degree-Of-Freedom attitude dynamics simulation called Tester. This model used the orbit history generated in the ballistic coefficient study to drive an attitude dynamics simulation. Since STK HPOP has high fidelity drag models available, density was also available as an input to Tester. Using the STK results, it was possible to recreate to a high degree of accuracy the perturbing forces that create environmental torques on NSD. This includes the gravity gradient, aerodynamic, and solar perturbing forces.

By contrast, the attitudes and attitude rates of the NSD are unavailable. A spin rate can be estimated at times from optical ground observations but attitude data is limited to approximations based on engineering judgment and sailcraft geometry. Studies have been conducted that combine estimates of starting spin rate and attitude with high-fidelity models of perturbing torques to attempt to establish limits on the offset between the Center of Pressure (CP) and Center of Gravity (CG) of the NSD and match the average solar area derived from the orbit simulation.

IV. Models

To model the aerodynamic and solar perturbation forces, we used STK HPOP. The drag model used the default STK drag coefficient (CD) of 2.20 along with the NRL MSISE atmospheric model and daily solar activity values obtained from the STK website. The SRP model in HPOP used 1.88 as an input for the pressure coefficient. In both cases, the area/mass ratio was varied to match the observed orbit behavior. The analysis was performed in 10-day segments, with a few smaller time increments analyzed for periods of interest such as full sun. A 10-day increment was a sufficient time increment to match the orbit within a prescribed tolerance. The as-flown TLE vectors were available on a roughly daily basis. The 10-day increments were times in which the solar and aero area/mass ratios were varied in STK HPOP.

We also developed a 3-DOF attitude dynamics simulation in Matlab called Tester. The 3-DOF rigid body dynamics model solved the equation:

$$I \cdot \alpha + \omega \times (I \cdot \omega) = \tau \tag{1}$$

In Eq. (1) I is the moment of inertia tensor, α represents the rotation acceleration vector; ω is the angular velocity vector; and τ is the sum of the disturbance torque vectors. Aerodynamic drag, solar radiation pressure, and gravity torques were modeled. Drag force is calculated through the equation:

$$f_{drag} = \frac{1}{2}\, \rho\, v^2\, Cd\, A \tag{2}$$

Eq. (2) illustrates aerodynamic drag's dependency on density ρ, satellite velocity v, and A – the reference drag area. Cd represents the Co-efficient of drag. Solar force is calculated through the equation:

$$f_{solar} = c_r \frac{2\,S\,We}{c} \left[\left(\frac{r_e}{r_s}\right)^2\right] \tag{3}$$

where c_r is coefficient of reflectivity, r_e is the average distance of earth from the sun, r_s is the distance of the sailcraft from the sun, S is the total sail area, We is the solar constant equal to 1368 $\frac{J}{sm^2}$, and c is the speed of light. STK HPOP uses c_r in the spherical SRP model that was used in this research. The 3-DOF attitude dynamics simulation used the more complex formulation of optical coefficients in McInnes [6].

The x, y, and z components of the gravity gradient torque are calculated through the equations [7]:

$$\begin{aligned} L_x &= \frac{3k}{R^3}\left[\left(I_{zz} - I_{yy}\right)a_y a_z\right] \\ L_y &= \frac{3k}{R^3}\left[\left(I_{xx} - I_{zz}\right)a_z a_x\right] \\ L_z &= \frac{3k}{R^3}\left[\left(I_{yy} - I_{xx}\right)a_x a_y\right] \end{aligned} \tag{4}$$

The variable k is the Earth gravitational parameter (the universal gravitational constant times Earth's mass), R is the orbital radius vector; I_{xx}. I_{yy}, I_{zz} are the inertial moments along the x, y, and z axes respectively, and a_x, a_y, and a_z are the direction cosines of R with respect to the body frame of the sail. L_x, L_y, and L_z are the gravitational torques in the body axis frame of the sailcraft.

All these torques were combined into Tester and Matlab ODE 45 was used to integrate the equations of motion as depicted in Eq. (1). The simulation was driven by orbit state vector data fit to the raw TLE data in STK HPOP.

V. Results

A. Drag Model Results

The results of the orbit decay study in STK HPOP are shown in Fig. 5. The STK predictions in blue align well with the TLE data in red. In HPOP we selected a detailed atmospheric model and daily values for solar activity, thus ensuring an accurate density. Referring to Eq. (2) above, the velocity was also well known from the orbit and the drag coefficient was always assumed to be 2.20, which is a reasonable approximation for a flat plate. Since optical ground observations established that the sailcraft was spinning at a rate far greater than the orbit rate, the drag area solved for in Eq. (2) and used with the area/mass ratio required by STK HPOP as an input can be

considered an average area over the orbit as the sailcraft spun. If it were possible to know the precise spin axis and rate of the sailcraft as a function of time, the drag could be modeled more accurately. However, Fig. 5 demonstrates that the assumption of an average cross-section for the sailcraft was more than sufficient to model the orbit decay.

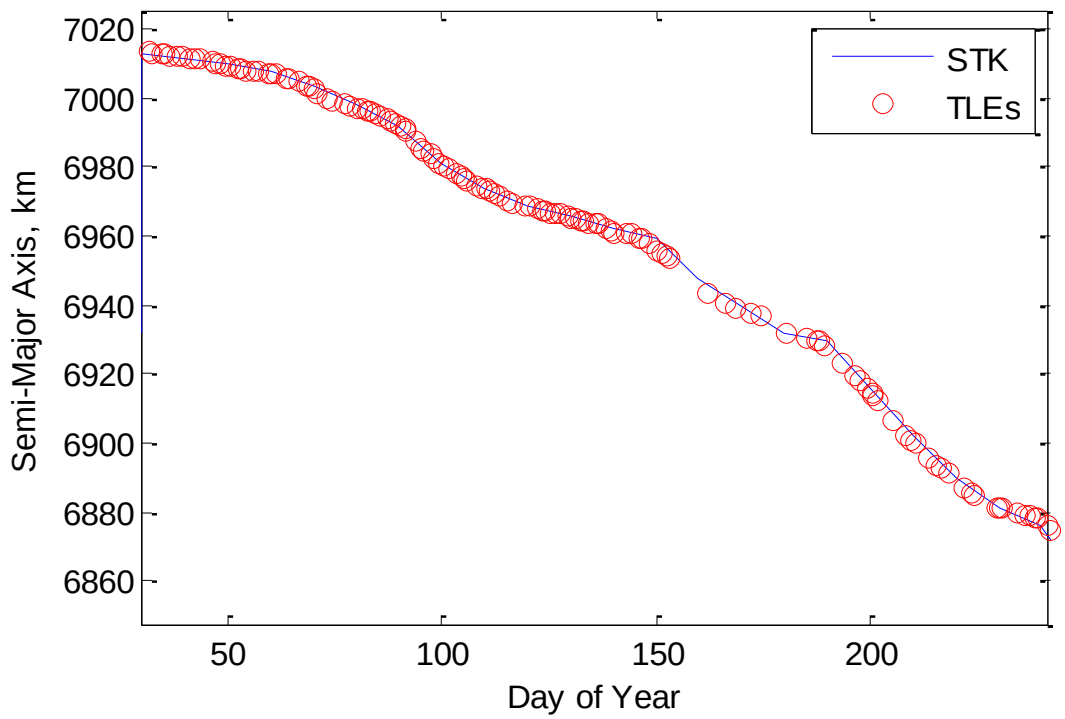

Fig. 5 Observed (TLEs) and Simulated (STK) Mean Semi-Major Axis

Over the course of the mission, TLE vectors were only available on a roughly daily basis with some gaps in coverage (a total of 167 in 240 days). In order to model the orbit decay, multiple observed state vectors are required for curve fitting of the mean Semi-Major Axis (SMA). Engineering judgment and trial and error led us to select a period of 10 days for each average cross-sectional drag area.

Thus the estimate of the drag area is based on an average fitted to TLEs over a period of 10 days and includes the rotation of the sailcraft relative to the inertial frame. Imagine that the sail is spinning and for a given orientation of the spin axis, the average area in the direction of the velocity vector can be estimated for purposes of calculating drag forces. That the area stayed more or less constant for periods of roughly 10 days could perhaps imply that the spin axis of the sailcraft for that time period was relatively constant.

In fact, the working hypothesis throughout this research was that the sailcraft may have approached a spin – stabilized condition at times. This is an assumption, but note that the sailcraft is axisymmetric about the Z axis (as

depicted in Fig. 2), and that it is well known from classical dynamics that an axisymmetric rigid body can be readily spin-stabilized [8].

To further explain the orbit geometry and disturbance torque environment during full sun conditions, Figures 6 and 7 show the orbit geometry for the full sun condition and the minimum sun condition.

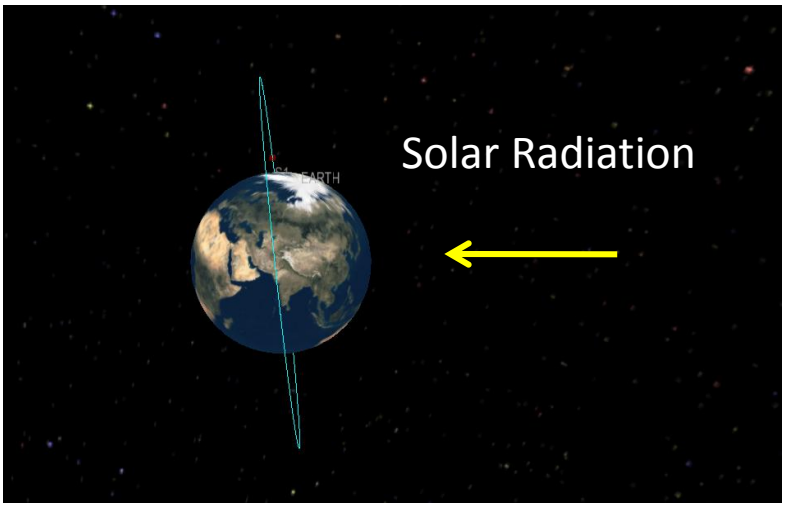

Fig. 6 Full Sun Orbital Geometry

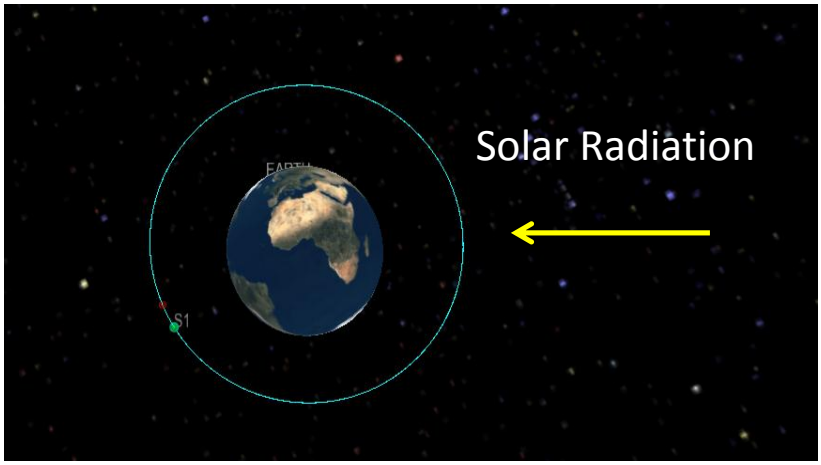

Fig. 7 Minimum Sun Orbital Geometry

From Fig. 6, one can deduce that the solar force will be roughly constant in the direction of the orbit angular momentum vector during the full sun condition. On the contrary, the orbit geometry in Fig. 7, where the solar direction is in the orbit plane, shows that in this case the solar disturbing force will constantly change direction over the course of an orbit. On the left and right of the plot in Fig. 7, the solar force will roughly be coincident with the positive and negative radius vector of the orbit. At the top and bottom the solar force is roughly coincident with the

negative and positive velocity vector of the orbit (assuming a clockwise rotation in the orbit plane of the sailcraft in its orbit). Thus it can be seen at a glance that the disturbance force environment in Fig. 6 is more consistent over an orbit than that in Fig. 7.

Other factors causing a difference between full sun and minimum sun are the presence of a shadow cone during the minimum sun period and the magnitude of the solar density over an orbit. For the shadow time, observe that on the left side of Fig. 7 there is a period when there is no solar force at all. Atmospheric density is also a strong function of orbital lighting [5]. Spot checking of STK HPOP density data showed that atmospheric density was a factor of 4-5 times higher between orbit midnight and orbit noon. But notice in Fig. 6 that since the orbit plane is almost perpendicular to the solar direction and the orbit is completely lighted, solar heating along the orbit is closer to constant and thus the density is also. Thus the drag force is less variable in Fig. 6 than it is in Fig. 7 over the course of an orbit.

Taking all these considerations into account, it is clear that the disturbance force direction and magnitude with respect to the orbit geometry is much more consistent over an orbit for the full sun condition as compared to the solar minimum. Thus, we might expect the sailcraft to tumble less, perhaps, in the full sun condition and so present a smaller effective drag area to the velocity vector.

To test this hypothesis, we closely examined the derived average drag area as a function of orbital lighting. Table 1 gives the result of this study by comparing β to average drag area at different times. β is used as a measure of sunlight exposure over the course of an orbit and is defined as the angle between the sun-earth line and the orbit plane. When the absolute value of β is near zero (Fig. 7) the sail orbit experiences the maximum shadow and minimum sun exposure. Conversely, when the absolute value of β is a maximum (Fig. 6), the sail can experience full sun for the duration of the orbit.

Table 1 shows a comparison of average drag over 10-day periods near both solar minimum and full sun conditions. There is a clear pattern of smaller average drag areas near solar maximum and vice versa. A smaller drag area could potentially imply a smaller spin precession axis during the full sun periods, or perhaps less tumbling of the sailcraft. The first ~ 40 days of the mission gave less consistent results, perhaps due to an initial "settling down" period for the sailcraft, lower aero forces or a combination of the two. Note also that due to the sun being in the northern hemisphere while orbit noon was in the southern hemisphere, the absolute value of β Day 160 was only 49 degrees, so that full sun did not occur, thus this period is called maximum sun.

Table 1 Average Drag Area in Full Sun and Minimum Sun Conditions

Days After Deploy	Condition	β (deg)	Area (meters^2)
76	Min Sun	0	5.34
105	Full Sun	88	2.04
135	Min Sun	0	5.77
160	Max Sun	-49	2.11
184	Min Sun	0	5.38
214	Full Sun	84	0.69

B. Solar Radiation Model Results

The average Solar Radiation Pressure (SRP) area can be determined in similar way. To model the solar radiation pressure, we examined argument of perigee and eccentricity, since those two parameters are the most sensitive to solar radiation pressure perturbation force. [5] Fig. 8 presents a plot of eccentricity over the course of the entire mission with respect to β.

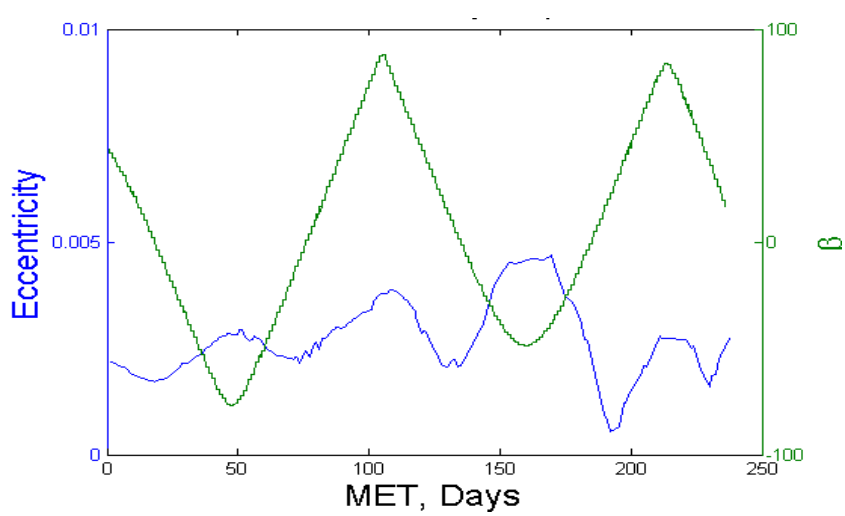

Fig. 8 Eccentricity and Beta Angle Comparison

Fig. 8 shows a clear correlation of eccentricity to β. Given the knowledge that argument of perigee and eccentricity are strongly affected by solar radiation pressure, we used these two elements to iterate for correct values

of average projected solar area over 10-day periods in the same way that drag area was derived using the observed mean SMA history.

In order to help determine the significance of solar radiation pressure on the NSD orbit, STK HPOP simulated the trajectory with and without the SRP model. The results of this simulation are presented in Fig. 9 for Argument of Perigee (AOP). In Fig. 9 the green line is the STK HPOP without SRP modeled, the red line is the same simulation with SRP modeled, and the blue dots are the AOP from the TLE data which was based on observations.

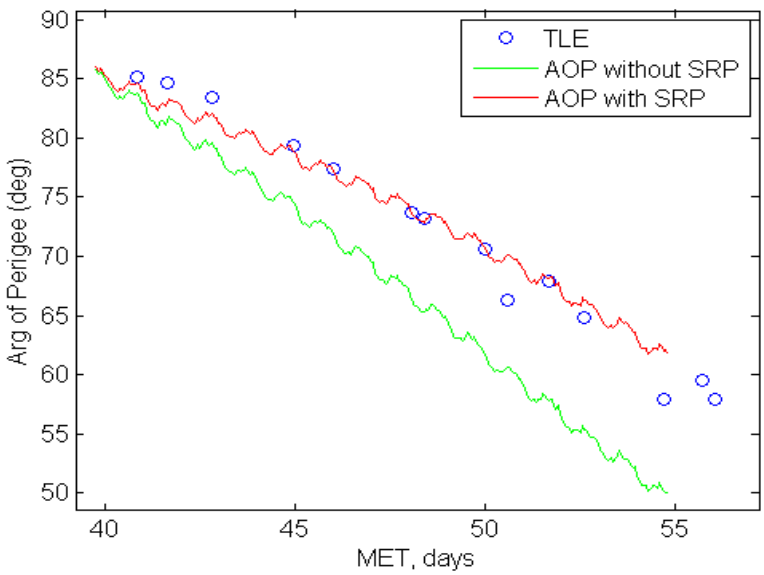

Fig. 9 Simulated AOP With and Without SRP Modeled

Some conclusions can be drawn from Fig. 9. First, the spherical model of SRP in STK HPOP is a good approximation of a spinning sailcraft provided the model is supplied with the correct reference area and radiation coefficient. For this study we used 1.88 for the radiation pressure coefficient in HPOP based on a simple average of the measured radiation pressure coefficients of the front (1.92) and back (1.83) of the NSD sail material. Note that the front and back coefficients are based on laboratory optical testing of the actual sail material that flew in space on NSD, since this material was carefully measured during the NASA In-Space Solar Sail Project [9]. Second, Fig. 9 demonstrates conclusively that the SRP effect on the orbit was significant and that the orbit could not be modeled accurately without an SRP model. Thus, NSD definitely demonstrated solar thrust that seemed to consistently be in a single direction roughly along the sail-sun line, even though it was spinning rapidly.

Table 2 SRP Area in Full Sun and Minimum Sun Conditions

Days After Deploy	Condition	β (deg)	Area (meters^2)
76	Min Sun	0	1.92
105	Full Sun	88	9.09
135	Min Sun	0	1.42
160	Max Sun	-49	4.61
184	Min Sun	0	4.68
214	Full Sun	84	6.91

Table 2 presents the results from STK HPOP that determined a best fit to SRP area for 10-day periods near solar minimum and full sun conditions. These values were selected by matching the simulated and observed eccentricity and AOP of the NSD orbit. The task was more difficult than matching the SMA decay rate. This difficulty was caused in part by the fact that eccentricity and AOP tend to be less well defined and noisier for low values of eccentricity and at times the eccentricity of NSD was below 0.01. Another reason that it was more difficult to match eccentricity and AOP compared to SMA is that although the spherical model of SRP in STK HPOP did a remarkably good job of modeling the optical properties of a spinning sailcraft, the limitation that the solar force acts only along the sailcraft-sun line undoubtedly still introduced some error.

Nevertheless, the values in Table 2 did provide a good fit to the eccentricity and AOP of the NSD orbit, as can be seen in Fig. 9. Keeping in mind that the goal of the research presented in this paper was to do a general characterization of the orbit and attitude dynamics of the NSD based on a limited set of flight data, the fit to the observed orbit parameters is surprisingly good considering the relatively sparse flight data available.

Based on heuristic insight, one might expect the effective or average solar area to increase during full sun conditions, and Table 2 displays exactly this pattern. As discussed above the local minimum of β was only -49 on Day 160 and full sun did not occur. It can be seen that the average solar area for the 10-day period around Day 160 was significantly lower than that of Day 105, but given the difference in the absolute value of the respective βs this is to be expected (this logic also applies to the drag area in Table 1, but that does not seem to have been affected as it is still comparable to the full sun drag areas). As expected, the solar area for solar minimums is generally much

smaller, although the solar area on Day 184 was larger than that of the two earlier solar minimum periods, perhaps because the atmospheric density was beginning to be the dominant disturbance force at this point in time.

The estimates of solar area give valuable information about the NSD and provide confirmation that the sail produced a significant thrust while spinning. Additionally the data in Table 2 also can assist with studies of the attitude dynamics of the NSD. To see this, refer to Fig. 10, which presents the definition of the Local Vertical Local Horizontal (LVLH) coordinate frame that is the one in general used by NASA. In this system of reference, the Y axis is aligned in the direction opposite the angular momentum vector of the orbit, the Z axis is in the opposite direction of the radius vector, and Y cross Z completes the triad in the general direction of the velocity vector.

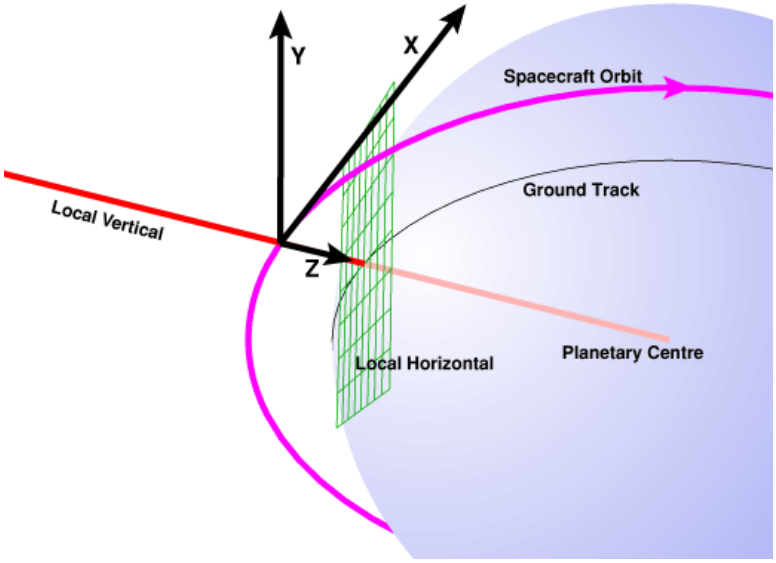

Fig. 10 LVLH Coordinate Frame

Consider the disturbance forces in the LVLH frame during a full sun condition. Since the orbit plane is nearly perpendicular to the sun, the solar pressure direction in the LVLH frame is then aligned mostly along the +/- momentum vector of the orbit (the +/- Y axis in Fig. 10) for the duration of the entire orbit. This is in contrast to the minimum sun condition when the solar disturbance force rotates between the +/- radial and +/- velocity directions (the +/-X and +/-Z axes in Fig. 10.) Given that in a full sun condition the solar force remains aligned with the angular momentum vector of the orbit, intuitively one might expect the sail to be “pushed into the orbit plane” by the solar torque. If this were the case, then one would also expect the sail to present a flatter aspect to the velocity

vector. The combination of these two effects would be to maximize solar area and minimize drag area when the sail is in a full sun condition. Table 1 and 2 confirm this heuristic reasoning very well, as they do indicate that the average 10-day solar areas and drag areas behave as expected during full sun. The gravity gradient and drag disturbance forces will always respectively be in the direction of the LVLH Z (or - radius) and LVLH X (or + velocity) and so will be consistent between full sun and minimum sun conditions.

The fact that the average solar and drag areas of the sail are somewhat predictable during full sun presents an opportunity to estimate a spin axis orientation (and thus a rough estimate of the attitude history) for the NSD during the time near full sun. Another piece of information that is relevant is that the NSD was axisymmetric and so the effect of the gravity gradient torque would tend to be to align the larger inertia axis (the axis with the bus or the body Z axis in Fig. 2) with the negative radius vector. Finally and fortuitously, there exist a few estimates of the spin rate of the NSD from ground observations, and two independent observations just days from the Day 160 maximum sun event.

C. Spin Rate Estimate from Optical Ground Measurements

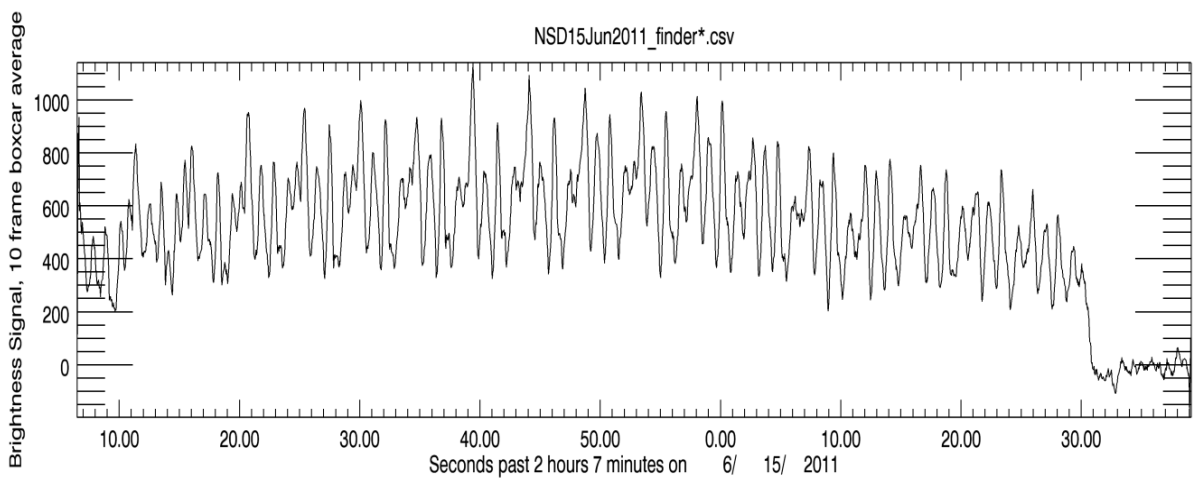

Fig. 11 Optical Brightness Measurement of NSD

Fig. 11 presents the results of an optical observation using a ground-based telescope at the Marshall Space Flight Center (MSFC) in Huntsville, Alabama by Dr. Robert Suggs. The information presented in Fig. 11 consists of

brightness measurements recorded during a pass of NSD over MSFC on June 15, 2011 (Day 165). Dr. Suggs also measured the brightness of NSD on June 13, 2011 (Day 163) and Ron Dantowitz of the Clayton Observatory Center in Boston, Massachusetts provided similar and independent data from measurements taken on June 8, 2011 (Day 158). Analysis of all three measurements by Dr. Suggs provided an estimate of approximately one rotation every 5 seconds which is equivalent to a spin rate of roughly 1.3 rad/sec. A close examination of Fig. 11 reveals smaller periodicities of four peaks per major cycle. The sub-peaks in amplitude clearly correspond to the four quadrants of the NSD, thus helping to confirm the estimate.

Optical observations were also achieved in mid-February and mid-August. The February observations estimated a rotation rate of once every 8 seconds or 0.8 rad/sec while the August observation estimated a rotation once every 3 seconds or 2.1 rad/sec. The spin rate of the NSD appeared to be increasing with time, perhaps due to the increasing atmospheric density as the altitude decreased.

D. Attitude Dynamics Simulation Results

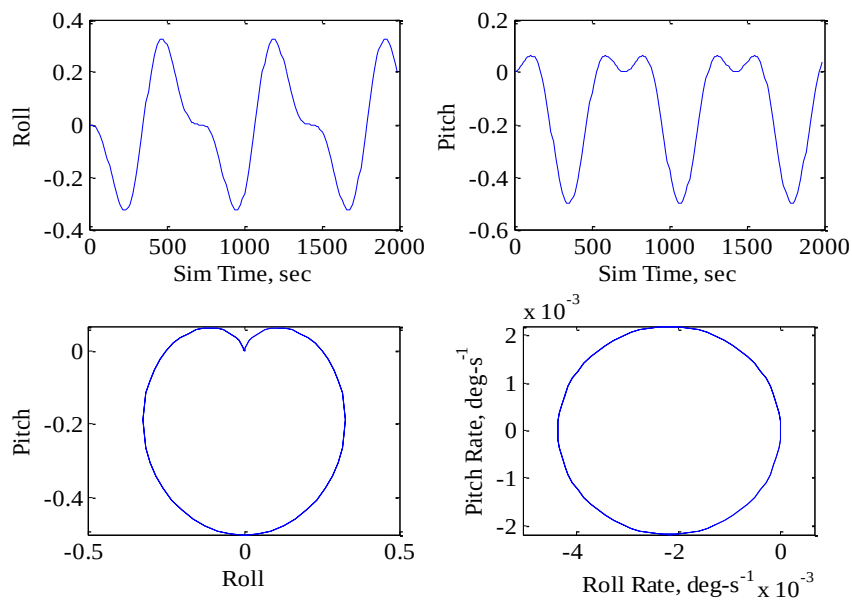

Fig. 12 Replication of Result from Wie

As discussed above, it's possible to derive a reasonable estimate of the NSD attitude around the time of the Day 160 solar maximum by combining STK-derived drag area and SRP area with the estimate of spin rate from the preceding section. This estimate can then be simulated in the 3-DOF attitude dynamics simulation Tester, which

takes the Best Estimate Trajectory (BET) from the STK results to provide high fidelity models of disturbance forces for use in environmental torque calculations.

Tester was developed in a modular fashion and tested as work proceeded. Each torque model was verified independently using idealized test cases to confirm the models were correct. The final verification was a comparison to a result in Wie [10]. The result of this simulation appears in Fig. 12 and is identical to Fig. 10 in Wie. It is worth noting that Wie's result was computed analytically while Tester solved the rigid body dynamics equations of motion numerically.

Using the average SRP and average drag areas from Tables 1 and 2, initial conditions to match those areas for the maximum sun condition of Day 160 and the full sun condition of Day 232 were estimated. For both of these days, estimates of spin rate based on ground observations were also available and these completed the initial conditions for Tester. Some selected results of these simulations are presented in Table 3.

Table 3 Attitude Dynamics Simulation Results

Days After Deploy	Mean Solar Area (meters^2)	Center of Pressure Offset (meters)
160	4.78	0.02
214	6.21	0.02

In Table 3, the mean solar area is the area averaged over one orbit of the spinning NSD that is perpendicular to the Sun-sail vector. The results show that the mean solar area was matched well compared to the results in Table 2. Once that result was matched with the values in Table 2, for both of the test cases a Center of Pressure (CP) offset from the geometric center of the sail was then varied. When the mean solar area predicted by the attitude dynamics simulation varied by a significant amount from the mean solar area in Table 3, then the value of CP was considered a rough upper limit on the size of a bias in the CP-CM offset on the sailcraft. Put another way, column 2 of Table 3 is the mean solar area for the simulation with no CP offset, and column 3 is an estimate of where the mean solar area deviates significantly from that in column 2. We also tracked the average drag area of the simulation, but it was not a primary focus.

For the results in Table 3, the matching of the average solar area is an indication that the estimate of spin rate and initial attitudes had some value. We do not claim to have replicated the precise attitude nor the exact spin axis of the

NSD, but the initial conditions were probably representative of the actual attitude and spin axis orientation on Days 160 and 214. The CP offset estimate should be considered more of a rough upper limit to the size of this parameter for NSD. The results were not completely unambiguous, and the time simulated and initial spin rates were varied from what was observed to aid a general understanding of the problem.

VI. Conclusions

The orbital and attitude dynamics of the NSD have been modeled based on a limited set of flight data. The simulations have produced an accurate model of the sail's orbit. The results of the orbit simulations produced estimates of mean solar area and drag area for 10-day increments of the mission. These estimates in combination with spin rate measurements from ground observations allowed initial conditions to be derived for an attitude dynamics simulation that correctly predicted the general observed behavior of the NSD mean solar area over one orbit during periods of full sun. The attitude simulations also led to a rough estimate of the CP bias from the geometric center of the sail, which is an important parameter for future sail missions.

In addition to the specific conclusions on the orbit and attitude dynamics of the NSD, simulation tools have been developed and honed that will aid future missions. The results of this research will directly aid verification work currently underway at NASA in support of the Sunjammer mission, the first controlled and instrumented American solar sail that is currently scheduled to be launched in November, 2014.

NSD also proved that a thin membrane of sail-like material with a large area/mass ratio is an excellent candidate for de-orbiting LEO satellites at the end of their lifetimes, which was one of its flight objectives. The attitude dynamics simulation results aid understanding the interplay between the solar and aerodynamic perturbing forces in LEO that will assist future mission designers who choose to use a sail-like device for de-orbiting satellites.

NSD achieved the first successful deployment of a solar sail for America, and the lessons learned from it are helping light the way to a bright future for solar sails.

Acknowledgements

We would like to acknowledge Dr. Robert Suggs and Rod Dantowitz for the optical measurements of the NSD and NASA for sponsoring the internships of Chelsea Katan and Brent Faller. We also acknowledge the NSD Principal Investigator, Dean Alhorn for his support and assistance during the NSD mission.

References

[1] Alhorn, D., Casas, J., Agasid, E., Adam, C., Laue, G., Kitts, C., O'Brien, S., "NanoSail-D: The Small Satellite That Could!", *AIAA/USU Conference on Small Satellites*, Logan, Utah, Aug. 2011, SSC11-VI-1.

[2] Whorton, M., Heaton, A., Pinson, R., Laue, G., Adams, C., "NanoSail-D: The First Flight Demonstration of Solar Sails for Nanosatellites", *AIAA/USU Conference on Small Satellites, Logan, Utah,* Aug. 2008, SSC08-X-1.

[3] Ellis, J., Lisano, M., Wolff, P., Evans, J., Bladt, J., Scheeres, D, Rios-Reyes, L., and Lawrence, D., "A Solar Sail Integrated Simulation Toolkit", *Proc. AAS/AISS Spaceflight Mechanics*, Maui, HI, Feb., 2004, AAS 04-283.

[4] Heaton, A., "GN&C Solar Sail Model Comparisons", *AIAA Guidance, Navigation and Control Conference*, Providence, Rhode Island, Aug., 2004, AIAA 2004-4890.

[5] Vallado, D., *Fundamentals of Astrodynamics and Applications,* Springer, 2007, New York, NY Chapter 8.

[6] Harris, M., *Spacecraft Gravitational Torques,* National Aeronautics and Space Administration. Langley, VA., 1969, NASA-SP 8024.

[7] McInnes, C., *Solar Sailing: Technology, Dynamics and Mission Applications*, Praxis Publishing Ltd.Chichester, 1999, UK, Chapter 2.

[8] Wertz, J. (Ed.), *Spacecraft Attitude Determination and Control*. Hingham, MA, 1978, D. Reidel Publishing Company, Inc.

[9] Nehls, M., "CP1 Environmental Effects Testing", NASA MSFC Technical Report, Sep., 2005.

[10] Wie, B., "Dynamic Modeling and Attitude Control of Solar Sail Spacecraft", NASA Solar Sail Technology Working Group (SSTWG) Final Report Jan. 10, 2002.